

## 비대칭 터빈 로터 실에 기인한 축 가진력

김우준\* · 송범호\*\* · 송성진\*\*\*

### Rotordynamic Forces Due to Rotor Sealing Gap in Turbines

Woo June, Kim\* · Bum Ho, Song\*\* · Seung Jin, Song\*\*\*

**Key words** : Sealing Gap, Excitation Force Coefficient, Unsteady, Whirling.

#### Abstract

Turbines have been known to be particularly susceptible to flow-induced self-excited vibration. In such vibrations, direct damping and cross stiffness effects of aerodynamic forces determine rotordynamic stability. In axial turbines with eccentric shrouded rotors, the non-uniform sealing gap causes azimuthal non-uniformities in the seal gland pressure and the turbine torque which destabilize the rotor system. Previously, research efforts focused solely on either the seal flow or the unshrouded turbine passage flow. Recently, a model for flow in a turbine with a statically offset shrouded rotor has been developed and some stiffness predictions have been obtained. The model couples the seal flow to the passage flow and uses a small perturbation approach to determine nonaxisymmetric flow conditions. The model uses basic conservation laws. Input parameters include aerodynamic parameters (e.g. flow coefficient, reaction, and work coefficient); geometric parameters (e.g. sealing gap, depth of seal gland, seal pitch, annulus height); and a prescribed rotor offset. Thus, aerodynamic stiffness predictions have been obtained. However, aerodynamic damping (i.e. unsteady aerodynamic) effects caused by a whirling turbine has not yet been examined. Therefore, this paper presents a new unsteady model to predict the unsteady flow field due to a whirling shrouded rotor in turbines. From unsteady perturbations in velocity and pressure at various whirling frequencies, not only stiffness but also damping effects of aerodynamic forces can be obtained. Furthermore, relative contributions of seal gland pressure asymmetry and turbine torque asymmetry are presented.

#### 1. Introduction

Over the years, various types of excitation mechanisms that induce rotordynamic instability, e.g., labyrinth seals and turbines, have been identified and analyzed (Den Hartog (1956), Thomas (1958), Alford (1965), Enrich (1976), Enrich and Childs (1984). A lumped parameter model for the flow inside a labyrinth seal cavity, with inlet and an exit, was initially developed by Kostyuk (1972). Then, Iwatsubo (1980) extended the model to account for the seal depth variation in an eccentric labyrinth seal by adopting harmonic solution approach. Furthermore, Millsaps (1994) experimentally and analytically examined unsteady aerodynamic effects in a whirling labyrinth seal in unshrouded turbine.

However less research has been conducted on the aerodynamic effects of non-axisymmetric sealing gaps in shrouded turbines. Therefore, this paper analyzes rotordynamic damping effects due to aerodynamic forces in an shrouded turbine with a whirling rotor. A new model developed from combination of Iwatsubo-Kostyuk seal model and Song and Martinez-Sanchez turbine model. The focus is on the physical mechanisms responsible for aerodynamic damping forces.

#### 2. Model Description

This section describes the model of a single stage shrouded axial turbine with a whirling rotor. The model is an incompressible, meridional plane analysis, examining rotordynamic characteristics due to aerodynamic forces. The details of the model has been described in Song & Song (2001), therefore only a brief description is presented here.

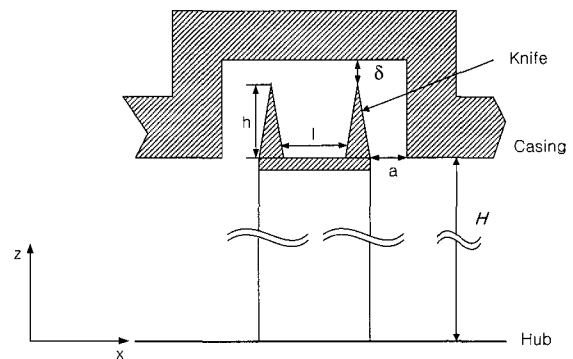
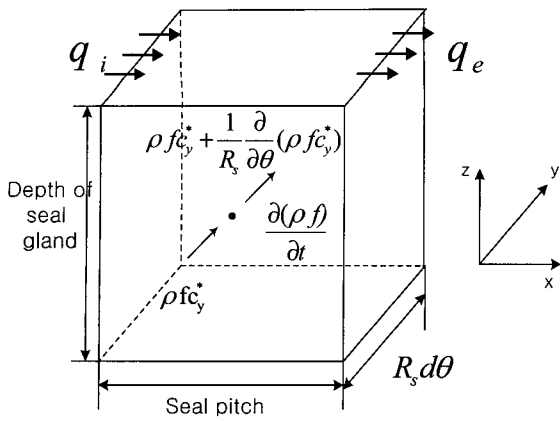


Figure 1. The components of labyrinth seal

\* 서울대학교 대학원, waiver2@snu.ac.kr

\*\* 르노삼성자동차, bhsong@renaultsamsung.com

\*\*\* 서울대학교 기계항공공학부, sjsong@snu.ac.kr



**Figure 2. Control volume with the associated mass fluxes.**

To analyze the seal flow, Millsaps' model (1994) has been adopted. A seal is shown schematically in Figure 1. The seal knife height is  $h$ , and the seal's length is  $l$ . The sealing gap is  $\delta$ , and the cavity depth is  $h + \delta$ . The leakage flow rate is affected mainly by the sealing gap  $\delta$  and the radial velocity of the leakage flow re-entering the annulus at the rotor exit is determined by the axial gap  $a$ .

Using Bernoulli equation and continuity, the following equations are obtained for seal leakage mass fraction,

$$\lambda = \frac{1}{c_{x0}} \frac{\delta_e \mu_e}{H} \sqrt{\frac{2(\delta_i \mu_i)^2}{(\delta_i \mu_i)^2 + (\delta_e \mu_e)^2}} \sqrt{\left(\frac{p_2 - p_3}{\rho}\right)^{-} + \frac{c_{x0}^2}{2}} \quad (1)$$

From the tangential momentum equation for the control volume, the following equation for  $c_y^*/c_{x0}$  can be obtained. Since the two friction factors also depend on  $c_y^*/c_{x0}$ , an iterative scheme is employed to solve for  $c_y^*/c_{x0}$ .

$$\begin{aligned} & \frac{1}{8} \left[ f_s \left( \frac{l}{H} + \frac{2a}{H} + \frac{2(h + \delta)}{H} \right) - f_r \left( \frac{l}{H} + \frac{4h}{H} \right) \right] \left( \frac{c_y^*}{c_{x0}} \right)^2 \\ & + \left[ \lambda + \frac{f_r}{4} \left( \frac{l}{H} + \frac{4h}{H} \right) \frac{U}{c_{x0}} \right] \frac{c_y^*}{c_{x0}} \\ & - \left[ \lambda \frac{c_{y2}}{c_{x0}} + \frac{f_r}{8} \left( \frac{l}{H} + \frac{4h}{H} \right) \left( \frac{U}{c_{x0}} \right)^2 \right] = 0 \end{aligned} \quad (2)$$

The following equation for  $AR$  is obtained from Bernoulli equation and axial momentum equation, where  $AR$  is area ratio.

$$\frac{1}{2} AR^3 + \left( \left( \frac{\lambda}{1 - \lambda} \right)^2 - \frac{3}{2} \right) AR^2 + \frac{3}{2} AR - \frac{1}{2} = 0 \quad (3)$$

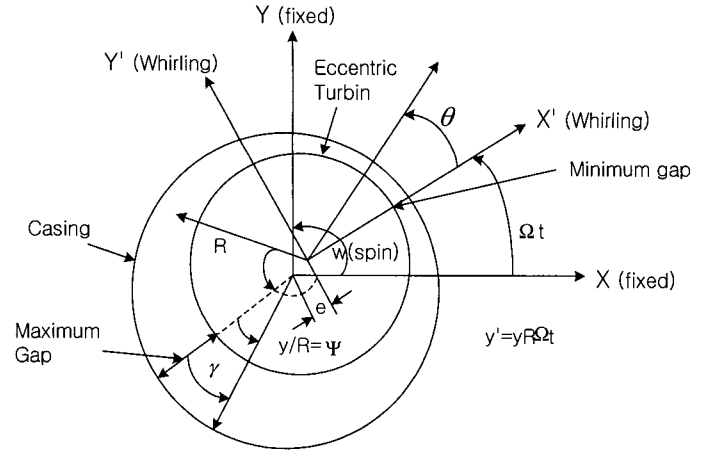


**Figure 3. Coordinate system used in the analysis**

For the main stream,  $(p_2 - p_3) / \frac{1}{2} \rho U^2$  is equivalent to the stagnation enthalpy drop, given by Euler's turbine equation, minus the kinetic energy gain.

$$\begin{aligned} \left( \frac{p_2 - p_3}{\frac{1}{2} \rho U^2} \right)^{-} &= \frac{c_{x0}}{U} \left[ \frac{c_{y2}}{c_{x0}} - \frac{c_{y3}}{c_{x0}} \right] \\ &+ \frac{1}{2} \left( \frac{c_{x0}}{U} \right)^2 \left[ \left( \frac{c_{x3}}{c_{x0}} \right)^2 + \left( \frac{c_{y3}}{c_{x0}} \right)^2 \right] \\ &- \frac{1}{2} \left( \frac{c_{x0}}{U} \right)^2 \left[ \left( \frac{c_{x2}}{c_{x0}} \right)^2 + \left( \frac{c_{y2}}{c_{x0}} \right)^2 \right] \end{aligned} \quad (4)$$

Then, the system of Eqs. (1), (2), (3) and (4) are solved simultaneously.

Figure 3 shows a turbine rotor simultaneously undergoing rotation and a circular whirl. Forward whirling direction is considered positive. The flow appears unsteady in inertial frame and steady in whirling frame. The azimuthal location the maximum tip gap is  $\Omega t + \pi$  radians from the inertial X axis. In the inertial frame, the rotor's whirling motion introduces unsteadiness:

$$\left( \frac{\partial}{\partial t} \right) = -\Omega R \frac{\partial}{\partial y} \quad (5)$$

The rotor offset,  $e$ , is assumed to be much smaller than the annulus is given by

$$\delta = \bar{\delta} + \text{Re} [ \hat{e} \exp[ i(y/R - \Omega t) ] ] \quad (6)$$

where  $\bar{\delta}$  is mean rotor sealing gap and  $y$  is the distance from the maximum tip gap in azimuthal direction.

From the perturbations in flow variables, lateral forces, or rotordynamic excitation forces, the total nondimensional lateral forces in the whirling frame  $X'Y'$  can be predicted.

$$\left[ \frac{F_y}{(Q/2r)(e/H)} + i \frac{F_x}{(Q/2R)(e/H)} \right] = \frac{-\hat{f}_y + iL\langle \hat{p} \rangle}{\hat{f}_y(e/H)} \quad (7)$$

Nondimensional damping and stiffness are extracted as follows: A plot of nondimensional whirling frequency can be curve fitted with a polynomial as follows:

$$\frac{F_y}{(Q/2R)(e/H)} = a + b \left( \frac{\Omega}{\omega} \right) + c \left( \frac{\Omega}{\omega} \right)^2 \quad (8)$$

where  $a=K_{xy}$  and  $b=-C_{xx}$ . Similarly, nondimensional direct force can be curve fitted as

$$\frac{F_x}{(Q/2R)(e/H)} = d + e \left( \frac{\Omega}{\omega} \right) + f \left( \frac{\Omega}{\omega} \right)^2 \quad (9)$$

where  $d=K_{xx}$  and  $e=-C_{xy}$ .

### 3. Model Predictions

This section presents the predicted nondimensional damping and stiffness for a selected turbine with a design flow coefficient, reaction, and work coefficient of 0.58, 0.208, and 1.5 respectively. This particular turbine has been selected because they describe the turbine tested by Song and Martinez-Sanchez (1997).

The design flow coefficient defined as the ratio of axial velocity to turbine rotational speed at the design condition and is representative of aerodynamic loading of turbine rotor blades - a lower value means higher loading. The focus is on the influence of design flow coefficient because it is arguably the most important turbine design parameter. Figure 4 shows the total nondimensional direct and cross forces vs the rotor whirling frequency for various  $\Phi_D$ 's. The cross force is more sensitive to the whirling frequency than the direct force. As described in the model description section, the lateral forces consist of pressure and torque asymmetries. Figures 5 and 6 show the breakdown of lateral forces in Figure 4 into those components. Pressure asymmetry decreases with increasing whirling frequency, but torque asymmetry remains almost same. Thus, the pressure asymmetry has the dominant influence on rotordynamic forces rather than the torque asymmetry.

Figure 7 illustrates the damping and stiffness coefficient plotted versus  $\Phi_D$ . According to Martinez-Sanchez et al (1995), the stability of a rotor system is determined by the direct damping coefficient  $C_{xx}$  and cross stiffness coefficient  $K_{xy}$ . The magnitudes of both  $C_{xx}$  and  $K_{xy}$  decreases nonlinearly as  $\Phi_D$  increases, and that trend is same to the unshrouded turbine. From a rotordynamic perspective, positive  $C_{xx}$  and  $K_{xy}$  values indicate stabilizing aerodynamic damping and destabilizing aerodynamic stiffness force, respectively. Decreasing  $\Phi_D$  leads to the penalty of higher  $K_{xy}$  but also yields the benefit of higher  $C_{xx}$ .

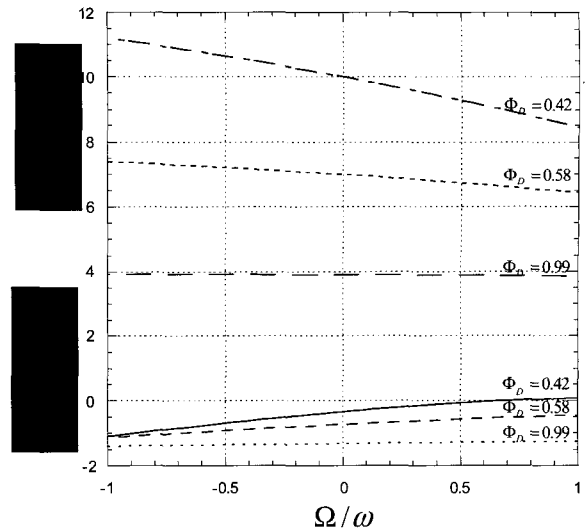


Figure 4. Total direct and cross stiffness vs whirling frequency for  $\Phi_D=0.42, 0.58,$  and  $0.99$ .

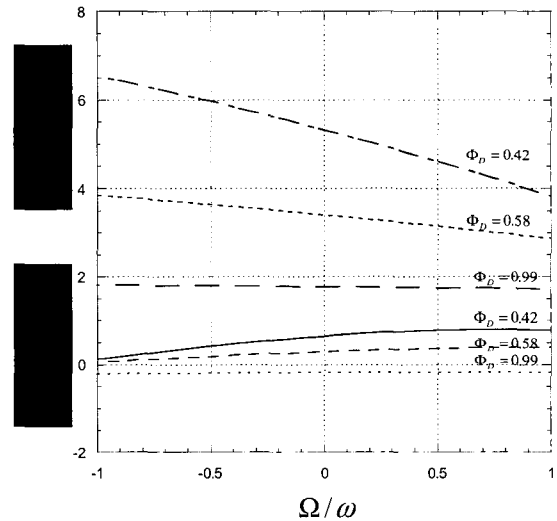


Figure 5. Direct and cross stiffness due to pressure asymmetry vs whirling frequency for  $\Phi_D=0.42, 0.58,$  and  $0.99$ .

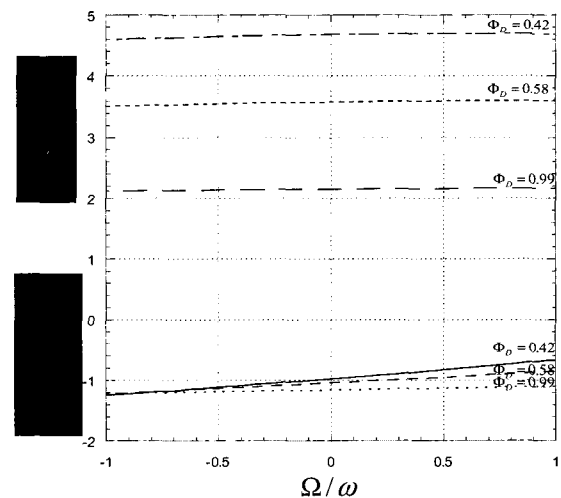


Figure 6. Direct and cross stiffness due to torque asymmetry vs whirling frequency for  $\Phi_D=0.42, 0.58,$  and  $0.99$ .

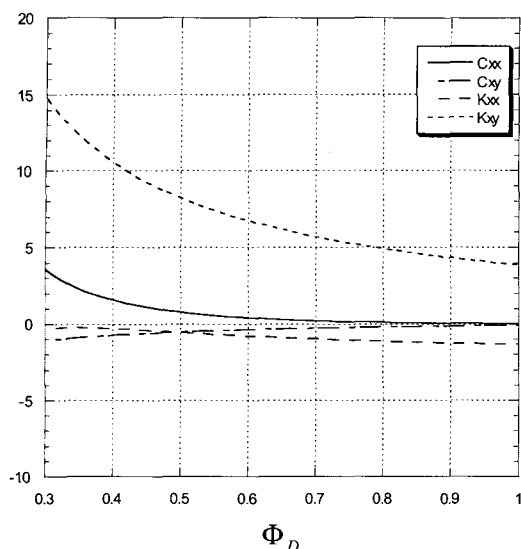


Figure 7. Damping and stiffness vs design flow coefficient.

#### 4. Conclusion

For the first time, the aerodynamic stiffness and damping forces caused by asymmetric tip clearance in an axial shrouded turbine with a whirling rotor have been analyzed. The focus is on the dynamic characteristics of the cross force. Furthermore, the dependence of such forces on the turbine design flow coefficient has been examined. The following conclusions can be made,

- 1) As the whirl speed increases, the cross force decreases in magnitude.
- 2) Pressure asymmetry has the dominant influence on rotordynamic force.
- 3) Increasing the design turbine loading, or decreasing the design turbine coefficient, leads to not only larger cross stiffness but also larger direct damping force.

#### 5. Acknowledgements

Support from the BK21 Project, sponsored by the Korean Ministry of Education, and the Micro Thermal System Research Center, funded by KOSEF, is gratefully acknowledged.

#### 6. References

- [1] Alford, J., 1965, "Protecting Turbomachinery From Self-Excited Rotor Whirl," ASME J. Eng. Power, Vol. 87, pp. 333~334.
- [2] Den Hartog, J. P., 1956, "Mechanical Vibrations," 4th edition, McGraw-Hill, New York, pp. 319~321.
- [3] Ehrich, F. F., 1976, "Self-Excited Vibration," Shock and Vibration Handbook, McGraw-Hill, 2<sup>nd</sup> Edition, pp. 1~5.
- [4] Ehrich, F. F., and Childs, D. W., 1984, "Self Excited Vibration in High Performance Turbomachinery," Mechanical Engineering, pp. 66~79.
- [5] Iwatsubo, T., 1980, "Evaluation of Instability Forces in Labyrinth Seals in Turbines or Compressors," NASA CP-2133, pp. 139~169.
- [6] Kostyuk, A. G., 1972, "A Theoretical Analysis of the Aerodynamic Forces in the Labyrinth Glands of Turbomachines," Teploenergetica, Vol. 19, No. 11, pp.29~33.
- [7] Martinez-Sanchez, M., Jaroux, B., Song, S. J., and Yoo, S., "Measurement of Turbine Blade-Tip Rotordynamic Excitation Forces," Journal of Turbomachinery, Vol.117, July 1995, pp. 384-393
- [8] Millsaps, K., and Martinez-Sanchez, M., 1994, "Dynamic Forces from Single Gland Labyrinth Seals: Part 1-Ideal and Viscous Decomposition," ASME Journal of Turbomachinery, Vol. 116, pp. 686 ~ 693.
- [9] Song B. H., and Song S. J., 2001, "Labyrinth Seal Effects in A Turbine Flow Field," ISABE Paper NO 2001-1227
- [10] Song, S. J., and Martinez-Sanchez, M., 1997, "Rotordynamic Forces Due to Turbine Tip Leakage: Part 1-Blade Scale Effects," ASME Journal of Turbomachinery, Vol. 119, pp. 695 ~ 703.
- [11] Song, S. J., and Martinez-Sanchez, M., 1997, "Rotordynamic Forces Due to Turbine Tip Leakage: Part 2-Radius Scale Effects and Experimental Verification," ASME Journal of Turbomachinery, Vol. 119, pp. 704 ~ 713.
- [12] Thomas, H. J., 1958, "Unstable Natural Vibration of Turbine Rotors Induced by the Clearance Flow in Glands and Blading," Bull. de l'A.I.M., 71, No. 11/12, pp. 1039-1063.